ACS Catalysis

pubs.acs.org/acscatalysis

Research Article

# Phenanthroline-Catalyzed Stereoselective Formation of α-1,2-*cis* 2-Deoxy-2-Fluoro Glycosides

Paul M. DeMent, Chenlu Liu,[†] Joseph Wakpal,[†] Richard N. Schaugaard,[†] H. Bernhard Schlegel,* and Hien M. Nguyen*

Cite This: *ACS Catal.* 2021, 11, 2108–2120

Read Online

ACCESS | Metrics & More | Article Recommendations | Supporting Information

**ABSTRACT:** Phenanthroline is a heterocyclic aromatic organic compound and commonly used in coordination chemistry acting as a bidentate ligand. The C4 and C7 positions of phenanthroline can often be substituted to change the binding capabilities of the ligand. Recently, there has been a push in the field of chemistry to create environmental-friendly chemical methodologies by utilizing catalysts and minimizing solvent. Herein, we have illustrated how, at high concentrations with minimal use of solvent, the C4 and C7 positions of phenanthroline can be tuned to develop an efficient and stereoselective catalyst for the formation of α-1,2-*cis*-fluorinated glycosides. By activating 2-deoxy-2-fluoro glycosyl halides with phenanthroline-based catalysts, we have been able to achieve glycosylations with high levels of α-selectivities and moderate to high yields. The catalytic system has been applied to several glycosyl halide electrophiles with a range of glycosyl nucleophilic acceptors. The proposed mechanism for this catalytic glycosylation system has been investigated by density functional theory calculations, indicating that the double $S_N2$ displacement pathways with phenanthroline catalysts have lower barriers and ensure stereoselective formation of α-1,2-*cis*-2-fluoro glycosides.

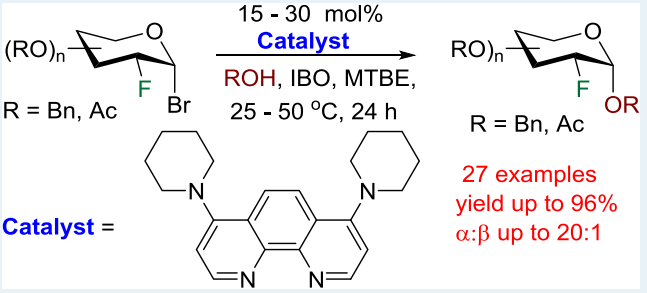


**KEYWORDS:** *catalytic glycosylation, stereoselective, phenanthroline catalyst, 1,2-cis-2-fluoro glycosides, oligosaccharides*



## INTRODUCTION

Carbohydrates are widespread in nature and have been considered as the frontier of medicinal chemistry.[1] In general, sugar-based biomolecules are constructed from rudimentary glycosylation reactions, which take place between a glycosyl donor (electrophile) and glycosyl acceptor (nucleophile).[2] These reactions allow for the establishment of two different α- and β-stereoisomers that differ in the configuration of the anomeric carbon. In many cases, α-glycosides have a cis relationship between the substituents on the anomeric carbon and the second carbon of the electrophilic coupling partner, with the exclusion of a few rare sugars. Conversely, β-glycosides would have a 1,2 trans relationship with the same exceptions.[3] By taking advantage of neighboring group participation of acyl protecting groups at the second carbon of glycosyl donor, 1,2-*trans* glycosides can be made with high levels of selectivity.[4] For this reason, many methods focus on the development of the stereoselective formation of 1,2-*cis* linked glycosides, which is the principal challenge of complex oligosaccharide synthesis.[5]

Although fluorine is the least abundant halogen present in natural products, it has been an essential element as a bioisotere of hydrogen and hydroxyl functionality in medicinal chemistry for the creation of new drugs and the improvement of existing ones.[6−10] Exchange of a hydrogen atom for a fluorine can impact the pharmacokinetics on the molecules, including p$K_a$, lipophilicity, binding affinity, and metabolic stability, without significantly altering the sterics of the molecule.[11] Currently, about 20% of the market pharmaceuticals contain at least one fluorine atom.[12] Even though both carbohydrates and fluorine play a significant role to the field of medicinal chemistry, there is a lack of methods for the stereoselective formation of fluorinated glycosides.[13,14] Recently, Gilmour and co-workers have established an effective methodology for selectively forming β-linked-fluorinated glycosides (Figure 1a).[15−18] The Gilmour approach is highly stereoselective toward β-1,2-*trans* glycosides. On the other hand, methodologies to selectively produce α-linked-fluorinated glycosides remain largely underdeveloped.

The ability of phenanthroline to effectively catalyze α-linked glycosidic bond formation when reacted with glycosyl bromides was recently discovered by our group.[19] This catalyst-controlled approach is highly predictable and provides

Received: October 9, 2020
Revised: January 21, 2021




https://dx.doi.org/10.1021/acscatal.0c04381
*ACS Catal.* 2021, 11, 2108–2120

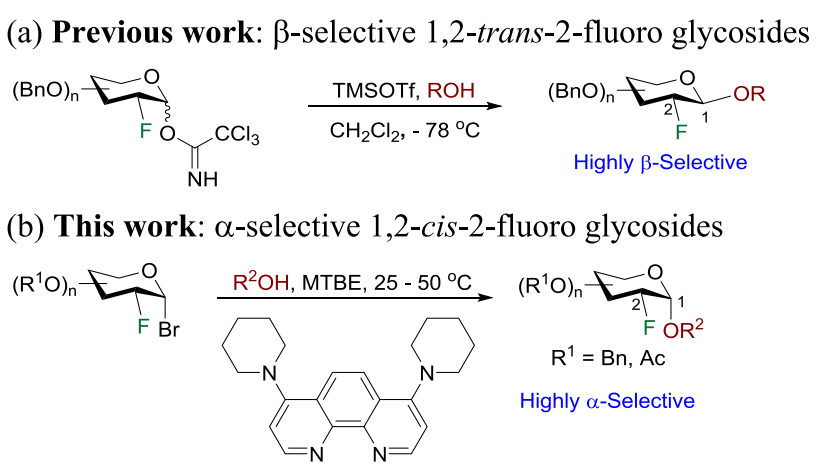


**Figure 1.** Stereoselective formation of $\alpha$- and $\beta$-fluorinated glycosides.

**Scheme 1. Preliminary Studies with Bathophenanthroline L1 Catalyst**

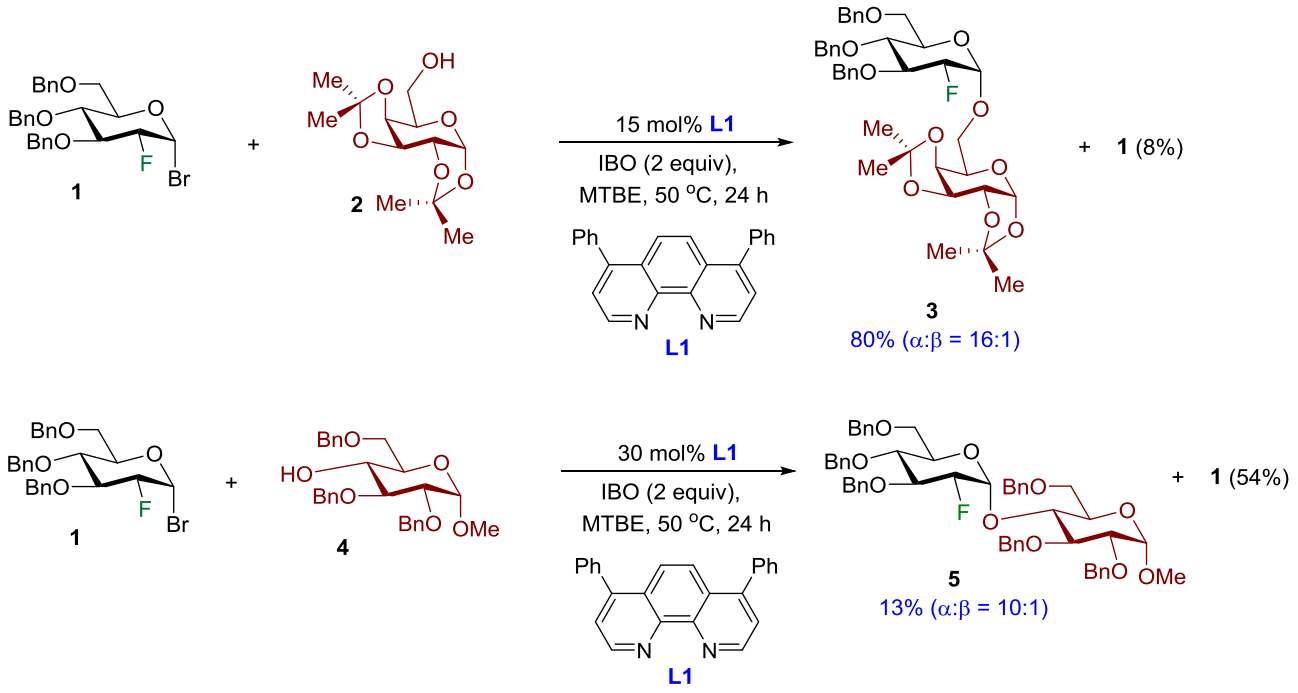


efficient access to a myriad of $\alpha$-1,2-*cis* glycosides. The phenanthroline-catalyzed glycosylation methodology mimics glycosyltransferase-catalyzed retentive mechanisms, wherein the stereochemistry of the products is influenced by the anomeric $\alpha$-configuration of glycosyl bromides. As a result, we question if this catalyst-controlled system gives an alternative stereochemical outcome of the inherently electronic bias of 2-fluoro substrates, providing efficient access to $\alpha$-1,2-*cis*-2-fluoro glycosides (Figure 1b). If successful, it will be complementary to the Gilmour's $\beta$-1,2-*trans*-2-fluoro glycoside approach. Herein, we illustrate that a wide range of $\alpha$-1,2 *cis* 2-fluoro glycosides can be stereoselectively accessed for the first time using commercially available and easily synthesized phenanthroline-based catalysts, $\alpha$-2-fluoro glycosyl bromides, and hydroxyl nucleophiles.

## RESULTS AND DISCUSSION

We initially investigated the reactivity of tribenzyl 2-fluoro glucosyl bromide **1** as an electrophilic coupling partner in the reaction with galactoside nucleophile **2** (Scheme 1) using our previously optimized conditions.[19] Accordingly, the glycosylation was performed with 15 mol % bathophenanthroline, **L1**, as a catalyst and isobutylene oxide (IBO) as acid scavenger of the HBr byproduct in methyl *tert*-butyl ether (MTBE) (0.5 M) at 50 °C for 24 h, and the desired fluorinated disaccharide **3** was effectively produced in good yield (80%) and $\alpha$-1,2 cis selectivity ($\alpha/\beta$ = 16:1). Encouraged by this result, we next investigated the coupling of the highly hindered C(4)-hydroxyl acceptor **4**. Although compound **4** displayed high levels of diastereoselectivity ($\alpha/\beta$ = 10:1), we observed low reactivity of this secondary alcohol. The desired disaccharide **5** was isolated in only 13% yield, along with the recovery of glucosyl bromide donor **1** (54%). This result became clear that the existing conditions were not effective at the coupling of the highly hindered acceptor with 2-fluoro glycosyl bromide donor.

The starting point of optimization was the identification of reaction parameters that could further improve the yield of the coupling product **5** (Table 1). Increasing the catalyst loading


https://dx.doi.org/10.1021/acscatal.0c04381
ACS Catal. 2021, 11, 2108−2120

**Table 1. Optimization of C4-Hydroxyl Tribenzyl Glycosides**[a,b,c]

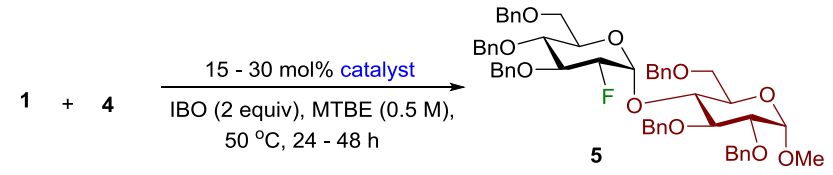


| entry | catalyst | loading (mol%) | 1 (equiv.) | 4 (equiv.) | time (h) | 5 yield (%)[b] | 5 (α:β)[c] | recovered 1 (%)[b] |
|---|---|---|---|---|---|---|---|---|
| 1 | L1 | 15 | 1 | 3 | 24 | 13 | 10:1 | 54 |
| 2 | L1 | 30 | 1 | 3 | 48 | 27 | 10:1 | 38 |
| 3 | L1 | 30 | 2 | 1 | 48 | 33 | 10:1 | 34 |
| 4 | L2 | 30 | 2 | 1 | 48 | Trace | - | 12 |
| 5 | L3 | 30 | 2 | 1 | 48 | 68 | 10:1 | 39 |
| 6 | L3 | 15 | 2 | 1 | 48 | 45 | 10:1 | 44 |
| 7 | L3 | 30 | 2 | 1 | 24 | 40 | 10:1 | 21 |
| 8 | L4 | 30 | 2 | 1 | 48 | 56 | 10:1 | 25 |
| 9 | L5 | 30 | 2 | 1 | 48 | 43 | 10:1 | 29 |
| 10 | L6 | 30 | 2 | 1 | 48 | 66 | 10:1 | 9 |
| 11 | L7 | 30 | 2 | 1 | 48 | 37 | 10:1 | 4 |
| 12 | L8 | 30 | 2 | 1 | 48 | 38 | 10:1 | 3 |
| 13 | L9 | 30 | 2 | 1 | 48 | 20 | 10:1 | 4 |

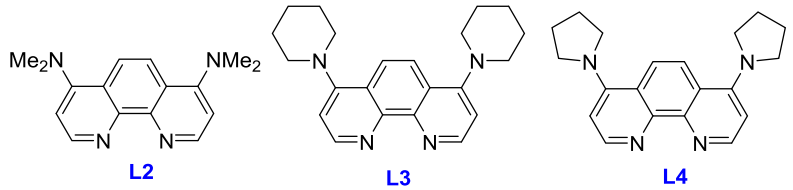

L2



L3



L4

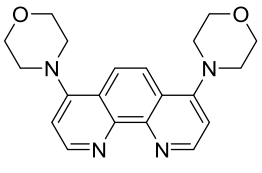

L5

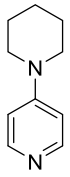

L6

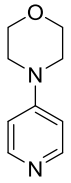

L7

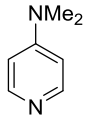

L8

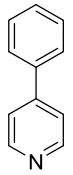

L9

[a]The reaction was conducted using 15−30 mol % catalyst **L1**−**L9**. [b]Isolated yield. [c]Diastereoselective ($\alpha/\beta$) ratio of the coupling product **5** determined by $^{19}$F nuclear magnetic resonance (NMR).

of **L1** and reaction temperature (entry 2) further improved the coupling efficiency, furnishing 27% of **5**. Further exploration revealed that switching the ratio of donor and acceptor slightly increased the yield of the coupling product (entry 3). Low conversion under **L1**-catalyzed glycosylation conditions with sterically hindered acceptor **4** appears to be likely due to the nucleophilic nature of the catalyst. With these observations in mind, several catalysts were investigated to determine the significance of the two nitrogen systems seen in bathophenanthroline, **L1**, and how changing the phenyl substituent at the C4 and C7 position can affect the glycosylation reactivity. First, it was decided to investigate a *N*,*N*-dimethylamino substituent (**L2**) in replacement of the C4- and C7-phenyl group. We hypothesized that switching to **L2** (entry 4) could further improve the yield because it is more nucleophilic than the **L1** catalyst due to the electron-donating nature of the *para*-substituted dimethylamino group. However, the reaction gave only trace reactivity (entry 4). In addition, significant side products were observed and glycosyl bromide donor **1** was recovered in only 12% yield. We hypothesized that the *N*,*N*-dimethylamino substituent could be acting as a competing nucleophile leading to the formation of many side products. To resolve this issue, we proposed that using a sterically hindered nitrogen at the C4 and C7 positions of phenanthroline could suppress these side reactions. To validate our hypothesis, the steric and electronic nature of the para-substituent, piperidine (**L3**), pyrrolidine (**L4**), and morpholine (**L5**) derivatives of phenanthroline were investigated (entries 5−9). Using the **L3** catalyst (entry 5) under analogous conditions showed the greatest improvement in yield (68%)


https://dx.doi.org/10.1021/acscatal.0c04381
ACS Catal. 2021, 11, 2108−2120

**Table 2. Reactions of Tribenzyl 2-Fluoro Glucosyl Bromide Using L1 and L3 Catalysts**[a,b,c]

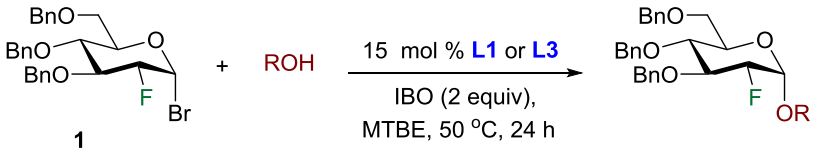


| entry | acceptors | products | results yield[b] (α/β ratio)[c] |
|---|---|---|---|
| 1 | 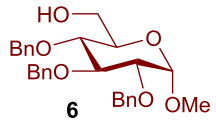 | 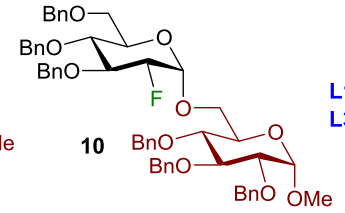 | L1: 62% (α:β = 7:1)<br>L3: 89% (α:β = 8:1) |
| 2 | 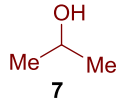 | 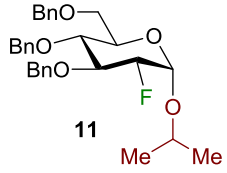 | L1: 52% (α:β = 7:1)<br>L3: 85% (α:β = 7:1) |
| 3 | 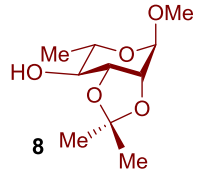 | 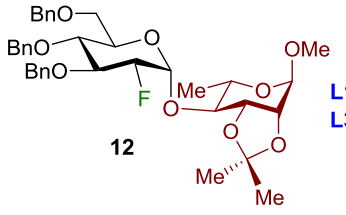 | L1: 42% (α:β > 20:1)<br>L3: 61% (α:β > 20:1) |
| 4 | 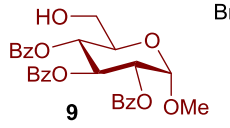 | 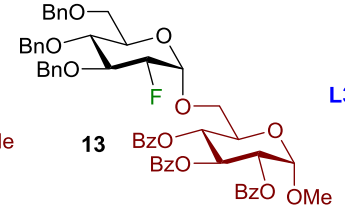 | L3: 85% (α:β = 7:1) |

[a]The reaction was conducted using 1 equiv of donor **1** and 3 equiv of acceptor. [b]Isolated yield. [c]Diastereoselective ($\alpha/\beta$) ratio of the coupling products determined by $^{19}$F NMR.

along with the preservation of glycosyl bromide starting material **1** (39%). Lowering the catalyst loading of **L3** (30 → 15 mol %, entry 6) resulted in no diminishment in selectively while decreasing the yield of the glycosylated product **5** (68 → 45%). Shortening reaction times (48 → 24 h) also diminished in yield (68 → 40%, entry 7).

To determine the importance of the dual nitrogen system displayed in the phenanthroline class, we next evaluated the corresponding pyridine type catalysts in promoting the glycosylations. The effects of the mononitrogen catalysts compared to the dual nitrogen catalysts on glycosylation efficiency are also illustrated in Table 1. Although both phenanthroline- and pyridine-derived catalysts provided disaccharide **5** with similar levels of selectivity ($\alpha/\beta$ = 10:1), it is noted by the consistently low amount of glycosyl bromide **1** recovered at the end of the reaction with the pyridine type catalysts (entries 10−13). For instance, while the 4-piperidine-substituted pyridine catalyst, **L6**, provided **5** in similar yield (66%, entry 10) to that the 4,7-piperidine-substituted phenanthroline catalyst **L3** (68%, entry 5), only 9% of starting material **1** was recovered for **L6** in comparison to 39% for **L3**. In all cases, the glucosyl bromide starting material **1** was recovered exclusively as $\alpha$-isomer.

With optimized conditions fully developed, the scope of the phenanthroline-catalyzed stereoselective coupling reaction was examined with a number of primary and secondary alcohols. We first focused on benzyl protected 2-fluoro electrophilic donors as they are known to be highly $\beta$-selective under the Gilmour's conditions.[15−18] Accordingly, the standard tribenzyl 2-fluoro glucosyl bromide **1** was evaluated with nucleophilic acceptors **6**−**8** to compare the efficiency of catalyst **L3** relative to catalyst **L1** (Table 2). The system employing **L3** uniformly furnished the coupling products **10**−**12** with higher yields compared to those using **L1**. In addition, our system relies on the phenanthroline catalyst to enforce stereocontrol of the newly formed glycosidic linkage. On the other hand, the Gilmour's methodology relies on the electronic bias of the 2-fluoro substrates to affect the stereoselective glycosidic bond formation.[15−18] For instance, the coupling of primary alcohol **6** with 2-fluoro glucosyl bromide **1** under **L3**-catalyzed


https://dx.doi.org/10.1021/acscatal.0c04381
ACS Catal. 2021, 11, 2108−2120

**Table 3. Reactions of Tribenzyl 2-Fluoro Galactosyl Bromide Using L1 and L3 Catalysts**[a,b,c,d,e,f]

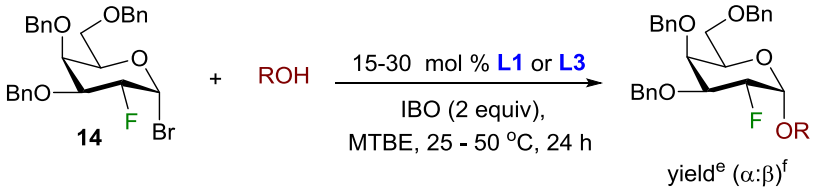


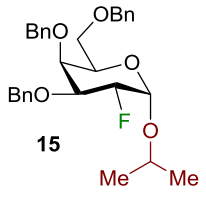


L1[a]: 50 °C, 80% (α:β = 3:1)
L1[a]: 25 °C, No reaction
L3[a]: 25 °C, 60% (α:β = 10:1)
L3[b]: 25 °C, 79% (α:β = 9:1)
L3[d]: 25 °C, 55% (α:β = 9:1)

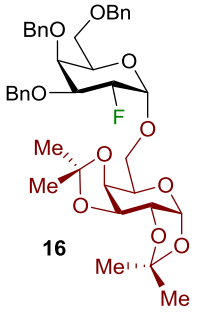


L1[a]: 50 °C, 76% (α:β = 4:1)
L3[c]: 25 °C, 75% (α:β = 12:1)

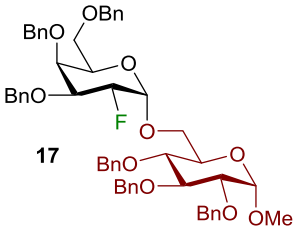


L1[a]: 50 °C, 63% (α:β = 3:1)
L3[a]: 25 °C, 85% (α:β = 11:1)

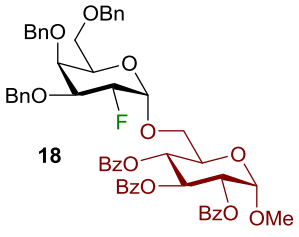


L3[a]: 50 °C, 80% (α:β > 20:1)

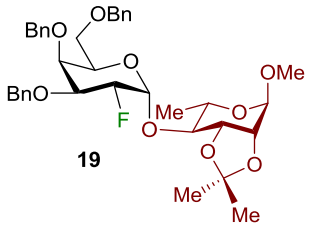


L1[a]: 50 °C, 35% (α:β = 8:1)
L3[a]: 50 °C, 81% (α:β = 8:1)

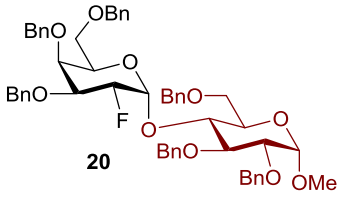


L1[b]: 50 °C, 38% (α:β = 9:1)
L3[c]: 50 °C, 75% (α:β = 10:1)

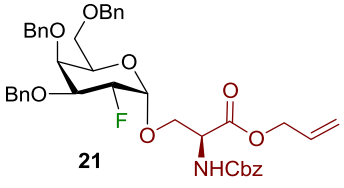


L1[a]: 50 °C, 80% (α:β = 3:1)
L3[b]: 25 °C, 73% (α:β = 7:1)

[a]The reaction was conducted using 15 mol % **L1** or **L3** at 0.5 M concentration for 24 h. [b]The reaction was conducted using 15 mol % **L1** or **L3** at 0.5 M concentration for 48 h. [c]The reaction was conducted using 30 mol % **L1** or **L3** at 0.5 M concentration for 24 h. [d]The reaction was conducted using 15 mol % **L3** at 0.2 M concentration for 48 h. [e]Isolated yield. [f]Diastereoselective ($\alpha/\beta$) ratio of the coupling products determined by $^{19}$F NMR.

conditions provided the desired disaccharide **10** with high $\alpha$-selectivity ($\alpha/\beta$ = 8:1, entry 1). In contrast, the Gilmour's method provided **10** with excellent levels of $\beta$-selectivity ($\alpha/\beta$ = 1:74).[15] Similarly, high $\alpha$-selectivity was also observed for secondary alcohols **7** and **8** (entries 2 and 3) with use of **L3** as a catalyst, while the Gilmour's method favors the $\beta$-diastereoselectivity for these acceptors.[15] Next, we examined the efficacy of this method to promote the coupling with electron-withdrawing alcohol nucleophile **9** (entry 4). Under **L3**-catalyzed optimized conditions, electron-poor acceptor **9** is well tolerated to furnish disaccharide **13** in comparable yield and selectivity (entry 4, **13**: 85%, $\alpha/\beta$ = 7:1) to the reaction with electron-donating alcohol **6** (entry 1, **10:** 89%, $\alpha/\beta$ = 8:1).

Reactivity of galactosyl bromide **14** with different glycosyl acceptors was next investigated utilizing catalysts **L1** and **L3** (Table 3) at a high (0.5 M) concentration. In many cases, the replacement of catalyst **L1** with catalyst **L3** results in improvement in both $\alpha$-selectivities and yields of the coupling products. It was significant to note that galactose donor **14** is more reactive than its glucose counterpart **1** as reactions can take place at ambient temperature with use of catalyst **L3**. For instance, glycosylation of isopropanol **7** with tribenzyl 2-fluro galactosyl bromide **14** using **L1** did not take place at 25 °C. In contrast, the use of **L3** proceeded smoothly at 25 °C under optimized conditions to afford the glycoside product **15** in 60% yield. The yield of the coupling product **15** was further improved (60 → 79%) when the reaction was allowed to stir for 48 h. Importantly, $\alpha$-selectivity improved 3-fold (**15**: $\alpha/\beta$ = 3:1 → 10:1) when the catalyst was switched from **L1** to **L3**. This significant improvement in diastereoselectivity is also observed with other hydroxyl acceptors (**2** and **6**), affording fluorinated disaccharides **16** ($\alpha/\beta$ = 4:1 → 12:1) and **17** ($\alpha/\beta$ = 3:1 → 11:1). To determine the effect of concentration on the reaction rate and selectivity, the coupling of isopropanol **7** with galactosyl bromide **14** was conducted at a lower concentration (0.2 M); fluorinated glycoside **15** was obtained in comparable selectivity ($\alpha/\beta$ = 9:1) to that obtained from the reaction conducted at a higher concentration (0.5 M), albeit in lower yield (79 → 55%). Under **L3**-catalyzed glycosylation conditions, the use of electron-withdrawing alcohol acceptor **9** proceeded sluggishly at room temperature and only 30% conversion was observed for the desired disaccharide **18**. We were pleased to find that **18** was obtained with a much higher


https://dx.doi.org/10.1021/acscatal.0c04381
ACS Catal. 2021, 11, 2108−2120

**Scheme 2. Glycosylation with 2-Fluoro Mannosyl Halides**

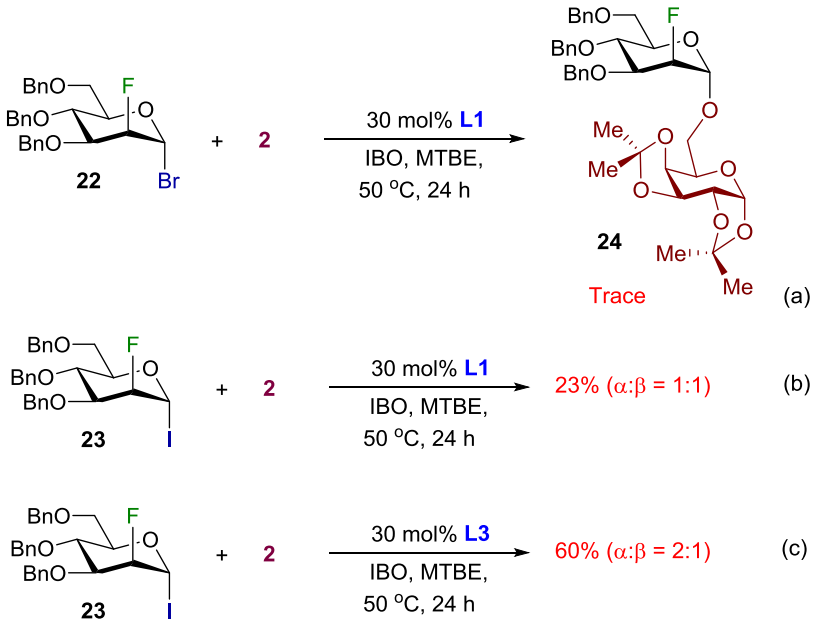


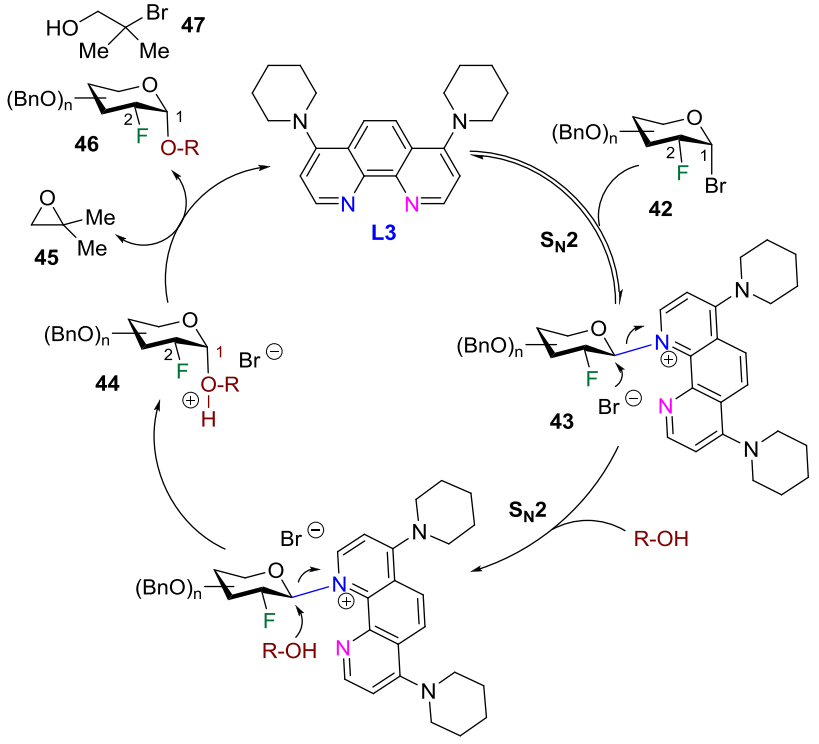


**Figure 2.** Proposed catalytic cycle of **L3**-catalyzed formation of $\alpha$-1,2-*cis*-2-fluoro glycosides.

yield (80%) and excellent $\alpha$-selectivity ($\alpha/\beta$ > 20:1) when the reaction was conducted at 50 °C. When highly hindered alcohols **4** and **8** were employed, the yield of the desired disaccharides **19** (35 → 81%) and **20** (38 → 75%) was significantly improved switching from **L1** to **L3**. Furthermore, we were encouraged by the observation that, under these optimized conditions, a significant increase in selectivity ($\alpha/\beta$ = 3:1 → 7:1) was observed with the use of serine amino acid to afford glycoconjugate **21**. In addition, the coupling proceeded smoothly at room temperature with the use of **L3** to afford **21** in 73% yield. To compare, the Gilmour's method is also highly $\beta$-selective for tribenzyl 2-fluoro galactose substrate.[16]

Unlike glucose **1** and galactose **14** bromide donors, 2-deoxy-2-fluoro mannosyl bromide **22** (Scheme 2a) is extremely stable and rather unreactive. For instance, the reaction gave trace reactivity with the use of **22** as a glycosyl donor in the coupling to galactoside acceptor **2** (Scheme 2a). Traditionally, glycosyl iodides have been utilized to increase the reaction rates of unreactive substrates.[20−25] As a result, the reactivity of the 2-fluoro mannosyl iodide **23** was evaluated (Scheme 2b). This change in leaving group improved the yield of disaccharide **24**


https://dx.doi.org/10.1021/acscatal.0c04381
ACS Catal. 2021, 11, 2108−2120

**Table 4. Glycosylation with 2,6-Dideoxy 2-Fluoro L-Glucosyl Bromides**[a,b,c]

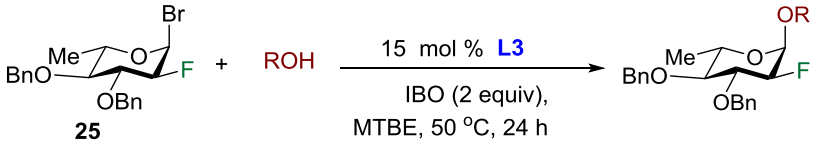


| entry | acceptors | products | yield[b] | α/β[c] |
|---|---|---|---|---|
| 1 | 2 | 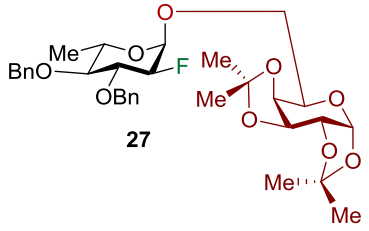 27 | 88% | >20:1 |
| 2 | 6 | 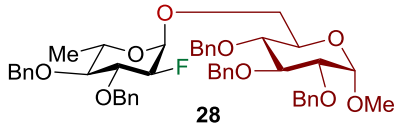 28 | 85% | 7:1 |
| 3 | 9 | 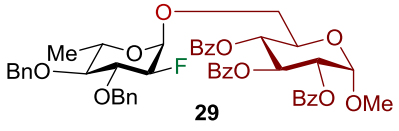 29 | 59% | 11:1 |
| 4 | 8 | 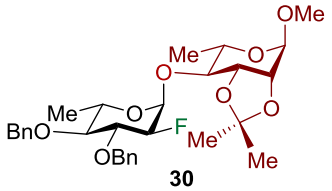 30 | 96% | >20:1 |
| 5 | 26 | 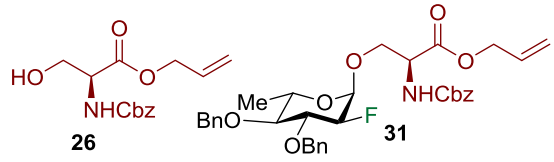 31 | 78% | 13:1 |

[a]The reaction was conducted using the **L3** catalyst. [b]Isolated yield. [c]Diastereoselective ($\alpha/\beta$) ratio of the coupling products determined by $^{19}$F NMR.

(trace → 23%), albeit with no selectivity ($\alpha/\beta$ = 1:1). When changing from **L1** to **L3** not only showed significant improvements in yield (23 → 60%) but diasteroselectivity also favors the $\alpha$-product **24** (Scheme 2c). This result underscores the distinct feature of the **L3** catalyst to increase the reaction reactivity and control diastereomeric outcome. In our proposed catalytic cycle (Figure 2), a double $S_N2$ pathway involves phenanthroline-catalyzed reaction with $\alpha$-glycosyl bromide. However, the $S_N1$−$S_N2$ reaction paradigm was shifted to favor the $S_N1$ pathway for the 2-fluoro mannose donor **23**.[5] As a result, poor diastereoselectively ($\alpha/\beta$ = 2:1) was observed for the product **24**. To compare, the Gilmour's methodology also shows poor selectivity and slightly favors $\beta$-diastereomer ($\alpha/\beta$ = 1:3.2) for the product **24**.[15]

2,6-Dideoxy sugars are important motifs of a variety of potent antibacterial and antitumor natural products.[26] Replacing a hydrogen atom at C(2) with a fluorine atom in 2,6-dideoxy sugars could facilitate the discovery of new potential antibiotics. In addition, a recent report illustrates that the coupling with 2,6-dideoxy-2-fluoro-L-glucose donors is highly $\beta$-selective under Gilmour conditions.[18] We question whether the **L3** catalyst could be highly $\alpha$-stereoselective toward the 2,6-dideoxy-2-fluoro substrate. Due to the highly reactive nature of dideoxy substrates, we explored the coupling of C6-hydroxyl galactoside acceptor **2** with 2,6-dideoxy-2-fluoro-L-glucosyl bromide **25** in the presence of 15 mol % **L3** at ambient temperature for 24 h (Table 4). The reaction proceeded smoothly to provide the desired disaccharide **27** (entry 1) in 88% yield with excellent levels of $\alpha$-selectivity ($\alpha/\beta$ > 20:1). Interestingly, switching to the C6-hydroxyl glucoside acceptor **6** reduced the selectivity of the coupling product **28** ($\alpha/\beta$ = 7:1, entry 2). Next, we investigated the glycosylation of electron-withdrawing acceptor **9** (entry 3) with donor **25** to determine how this nucleophile compared to


https://dx.doi.org/10.1021/acscatal.0c04381
ACS Catal. 2021, 11, 2108−2120

**Table 5. Glycosylation with Triacetyl Glycosyl Bromides**[a,b,c,d,e]

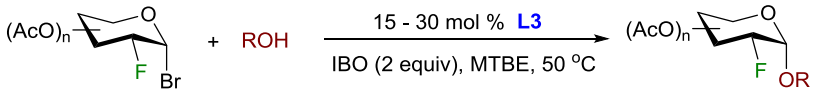


| entry | donors | acceptors | products | yield[c] (α/β ratio)[d] |
|---|---|---|---|---|
| 1 | 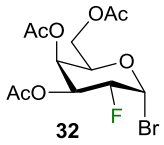 **32** | 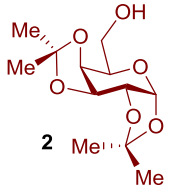 **2** | **35** | 64% (α:β = 7:1)[a] |
| 2 | **32** | 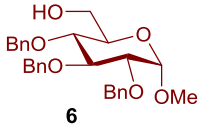 **6** | **36** | 70% (α:β = 9:1)[b] |
| 3 | 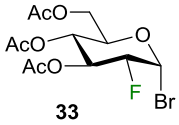 **33** | **6** | **37** | 72% (α:β = 7:1)[b] |
| 4 | **33** | **2** | **38** | 67% (α:β = 10:1)[b] |
| 5 | 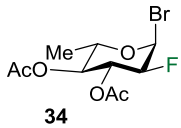 **34** | **2** | **39** | 76% (α:β = 11:1)[c] |
| 6 | **34** | **6** | **40** | 85% (α:β = 8:1)[a] |
| 7 | **34** | 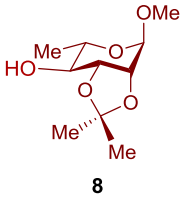 **8** | **41** | 52% (α:β = 20:1)[c] |

[a]The reaction was conducted using 15 mol % **L3** for 48 h. [b]The reaction was conducted using 30 mol % **L3** for 48 h. [c]The reaction was conducted using 30 mol % **L3** for 24 h. [d]Isolated yield. [e]The $\alpha/\beta$ ratio of the coupling products determined by $^{19}F$ NMR.

its electron-rich counterpart **6**. Gratifyingly, we observed that this electron-deficient alcohol **9** was equally competent to provide disaccharide **29** (entry 3) in 59% yield with high diastereoselectivity ($\alpha/\beta$ = 11:1). Encouraged by these results, we examined a more challenging C4-hydroxyl acceptor **8**. To our excitement, disaccharide **30** (entry 4) was isolated in excellent yield (96%) and $\alpha$-selectivity ($\alpha/\beta$ > 20:1). Protected serine amino acid residue **26** (entry 5) was also well tolerated under **L3**-catalyzed conditions to provide glycoconjugate **31** in good yield (78%) and high diastereoselectivity ($\alpha/\beta$ = 13:1).

Having probed the effect of benzyl protected 2-fluoro bromide donors **1**, **14**, and **25** in the reaction with a broad range of alcohol coupling partners with the use of **L1** and **L3** catalysts, we next investigated the impact of acetyl protected 2-fluorinated glycosyl bromide donors **32**−**34** (Table 5) on the glycosylation reactivity and selectivity. The Gilmour's method showed that substitution of the benzyl protecting group by the acetyl group on 2-fluoro glucose donor provided the product with only marginal $\beta$-selectivity ($\alpha/\beta$ = 1:21 → 1:2).[15] To determine the ability of the **L3** catalyst to overturn the substrate's inherent selectivity preference, acetyl protected 2-fluoro bromide donors **32**−**34** were coupled with a number of alcohols (Table 5) and compared to similar couplings with benzyl protected donors **1**, **14**, and **25** as well as the Gilmour's method.[15] The results obtained with acetyl protected donors **32**−**34** in Table 5 deserved comments. First, all glycosylations were conducted at 50 °C for 24−48 h. Second, acetyl protected donors **32**−**34** furnished coupling disaccharides **35**−**41** in good to excellent $\alpha$-selectivity under **L3**-catalyzed conditions. Third, although acetyl protected donors favor the


https://dx.doi.org/10.1021/acscatal.0c04381
ACS Catal. 2021, 11, 2108−2120

**Scheme 3. Control Experiments**

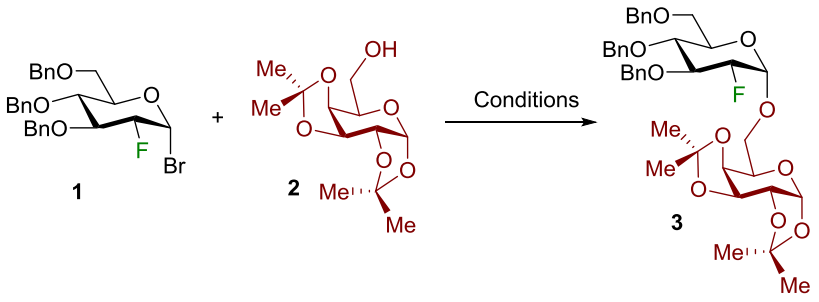


| Conditions | Results | |
|---|---|---|
| No Catalyst, IBO, MTBE, 50 °C, 24 h | Trace | (a) |
| AgOTf (1 equiv), DTBMP, $CH_2Cl_2$, 25 °C | 83%, α:β = 1:1 | (b) |
| 15 mol% **L3**, No IBO, MTBE, 50 °C, 24 h | 45%, α:β = 10:1 | (c) |

$\alpha$-selectivity, they are less diastereoselective than their benzyl counterparts. For instance, while the coupling of primary alcohol **2** with triacetyl galactose bromide **32** provided disaccharide **35** with $\alpha/\beta$ = 9:1 (Table 5, entry 1), the coupling of **2** with tribenzyl counterpart **14** provided disaccharide **16** with $\alpha/\beta$ = 12: 1 (Table 3). Fourth, in contrast to the Gilmour's method whose acetyl 2-fluoro donors provided the coupling products as a mixture of $\alpha$- and $\beta$-isomers,[15] the **L3**-catalyzed method selectively favors $\alpha$-products. For instance, **L3**-catalyzed coupling with triacetyl 2-fluoro glucose bromide **33** afforded disaccharides **37** and **38** (entries 4 and 5) with high diastereoselectivity ($\alpha/\beta$ = 7:1−10:1), while the Gilmour's method afforded the similar products with marginal $\beta$-selectivity ($\alpha/\beta$ = 1:2).[15] Finally, both acetyl- (**34**) and benzyl- (**25**) protected 2,6-dideoxy donors uniformly furnished the glycosylated products with high levels of diastereoselectivity. Overall, the results illustrate that the ability of the **L3** catalyst to control the $\alpha$-selectivity of newly formed glycosidic bonds regardless of whether electron-rich (Bn) or electron-deficient (Ac) protected 2-fluoro donors are employed in the reaction.

To illustrate that phenanthroline **L3** is not only a bond-forming catalyst but also enforces the stereoselective formation of $\alpha$-glycosidic bond, we conducted the reaction of glycosyl bromide **1** with nucleophilic acceptor **2** in the absence of the **L3** catalyst (Scheme 3a). As expect, only trace amount of the desired disaccharide **3** was observed. For comparison, we also performed the coupling utilizing silver triflate, AgOTf, as a Lewis acid (Scheme 3b), wherein the reaction often proceeds through an $S_N1$-like pathway, to provide a mixture of $\alpha$-1,2-cis- and $\beta$-1,2-trans products. As we anticipated, the use of a stoichiometric amount of AgOTf afforded disaccharide **3** as a 1:1 mixture of $\alpha$- and $\beta$-diastereomers. Furthermore, using isobutylene oxide (IBO) as a hydrogen bromide scavenger was beneficial to the yield. In the absence of IBO, the desired disaccharide **3** was isolated in only 45% yield (Scheme 3c).

On the basis of the aforementioned data, a proposed catalytic cycle for the phenanthroline-catalyzed formation of $\alpha$-1,2-*cis*-2-fluoro glycosides is illustrated in Figure 2. In the first step, the **L3** catalyst can engage in electrophilic activation of the bromide leaving group of glycosyl electrophile **42** to form the covalent $\beta$-glycosyl phenanthrolium intermediate **43** via an invertive $S_N2$ pathway. The glycosyl phenanthrolium ion formed in the reaction prefers the equatorial position to avoid the steric and electrostatic interactions associated with positioning that group in the axial orientation.[27−29] Subsequent $S_N2$ displacement of the phenanthrolium species **43** by an alcohol acceptor takes place in such a way that the stereochemistry of the protonated 2-fluoro glycoside product **44** would be dictated by the anomeric configuration of the phenanthrolium intermediate **43**. In the presence of isobutylene oxide (IBO) **45** as a hydrogen bromide scavenger, the $\alpha$-1,2-*cis*-2-fluoro glycoside **46** is ultimately generated with the regeneration of the **L3** catalyst. For certain coupling partners, the $S_N1-S_N2$ reaction paradigm was slightly shifted, wherein the covalent $\beta$-glycosyl phenanthrolium intermeidate **43** dissociate to form a transient oxocarbenium ion in the reaction. An alcohol nucleophile is then approached on either $\alpha$- or $\beta$-face of the oxocarbenium intermediate to provide the coupling product with a moderate $\alpha/\beta$ ratio.

To further gain insight into the mechanism, we attempted to detect a transient $\beta$-covalent phenanthrolinium ion (Figure 2) using NMR spectroscopy. Although we were not successful in detecting by NMR spectroscopy, a transient $\beta$-covalent phenanthrolinium intermediate with C2-*O*-benzyl functionality was detected by electrospray ionization (ESI) mass spectrometry.[19] This result suggests that the formation of the $\beta$-covalent phenanthrolinium intermediate is reversible. In addition, we previously observed that $\beta$-bromide only slowly anomerized to the corresponding $\alpha$-bromide without the phenanthroline **L1** catalyst.[19] However, $\beta$-bromide rapidly converted into $\alpha$-bromide in the presence of 15 mol % of **L1** catalyst within 1 h at ambient temperature and within 15 min at 50 °C.[19] We also previously conducted the coupling of $\beta$-anomer of glycosyl bromide with alcohol acceptor **2** in the presence of **L1**, and we observed that isomerization of $\beta$-bromide to $\alpha$-bromide is faster than the formation of the coupling product.[19] Coupling of acceptor **2** with $\beta$-isomer of glycosyl bromide under **L1**-catalyzed conditions provided the coupling product in comparable yield and $\alpha$-selectivity to that obtained with $\alpha$-isomer counterpart. Collectively, these results suggest that $\beta$-isomer of glycosyl bromide donor is not the reacting partner in the phenanthroline-catalyzed glycosylation reaction.

To determine that alcohol **47** (Figure 2) derived from isobutylene oxide (IBO) **45** is generated in the reaction and potentially reacts with the $\beta$-glycosyl phenanthrolium inter-


https://dx.doi.org/10.1021/acscatal.0c04381
ACS Catal. 2021, 11, 2108−2120

**Scheme 4. Detection of Alcohol 47 Derived from Isobutylene Oxide and Glycosyl Bromide**

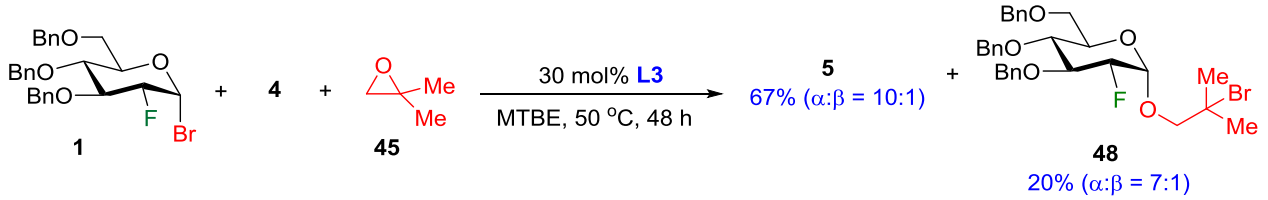


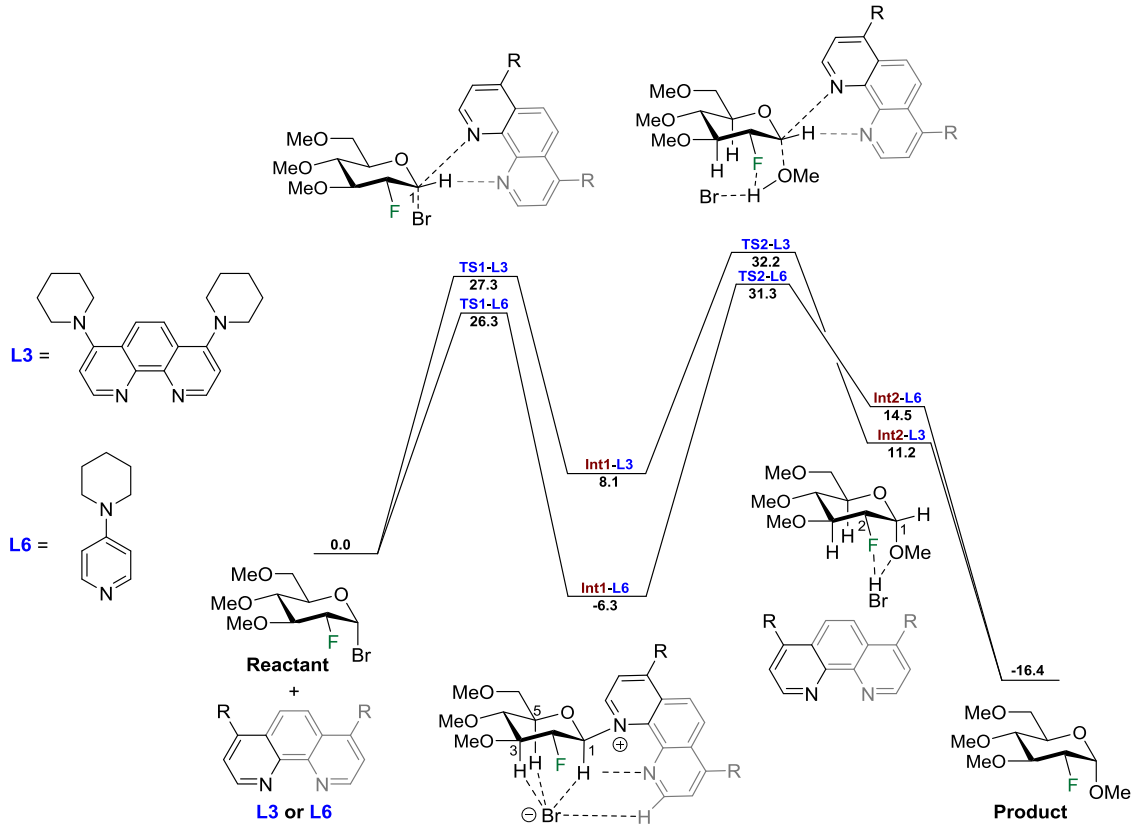


**Figure 3.** Energetic profile for the coupling of methanol with glycosyl bromide (**reactant**) to form $\alpha$-1,2-*cis* glycoside (**product**) using **L3** and **L6** catalysts and IBO as an HBr scavenger (units = kcal/mol).

mediate **43**, the coupling of sterically hindered C4-hydroxyl **4** with glucosyl bromide **1** (Scheme 4) was examined in the presence of IBO (**45**, 2 equiv). We chose **1** and **4** as coupling partners because we observed that alcohol **47** derived from IBO **45** did compete with sterically hindered nucleophiles. Accordingly, **L3**-mediated coupling of acceptor **4** with donor **1** proceeded at 50 °C to provide the desired disaccharide **5** and glycoside product **48**. The formation of **48** supports that alcohol **47** is indeed formed in the reaction and competes with nucleophilic acceptor **4** to react with a transient $\beta$-glycosyl phenanthrolium ion (Figure 2).

To provide further insight into the reaction mechanism that phenanthroline catalyst plays a key role in controlling the 1,2-cis selectivity and to understand the differences among the catalysts, density functional theory (DFT) calculations were used to examine the transition states and intermediates along the reaction pathway. The geometries of structures were optimized and vibrational frequencies were calculated with the B3LYP functional[29−33] and the Def2SVPP basis set[34] with the GD3BJ empirical dispersion correction[35,36] and the SMD implicit solvation model[37] for diethyl ether. Free energies were obtained by combining single-point calculations using the Def2TZPP basis set[38] at the Def2SVPP optimized geometries and zero-point energies. Thermal corrections and entropies were calculated with the Def2SVPP basis. Calculations were carried out with the Gaussian series of programs.[39]

The energy profile for the best catalysts, **L3** and **L6**, is shown in Figure 3. The results for the other substituted phenanthroline and pyridine catalysts (**L1**, **L2**, **L4**−**L9**) can be found in the Supporting Information, along with unsubstituted phenanthroline (**L0**) and pyridine (**L10**). The first step is an $S_N2$ displacement of bromide by the catalyst. For the phenanthroline catalysts (**L0**−**L5**), **L3** has the lowest barrier transition state 1, **TS1** (27.3 kcal/mol relative to separated reactants). It is observed that one phenanthroline nitrogen displaces the bromide leaving group while the other nitrogen is in close contact with the hydrogen on C1 of the sugar. Formation of the intermediate **Int1** follows with the displaced bromide interacting with the hydrogens on C1, C3, and C5 of the sugar and one of the phenanthroline hydrogens. This intermediate is 8.1 kcal/mol less stable than separated reactants. For the pyridine catalysts (**L6**−**L10**), the bromide of **Int1** interacts with the hydrogens on C1 of the sugar and C2 of the catalyst, and these intermediates are about 10 kcal/mol more stable


https://dx.doi.org/10.1021/acscatal.0c04381
ACS Catal. 2021, 11, 2108−2120

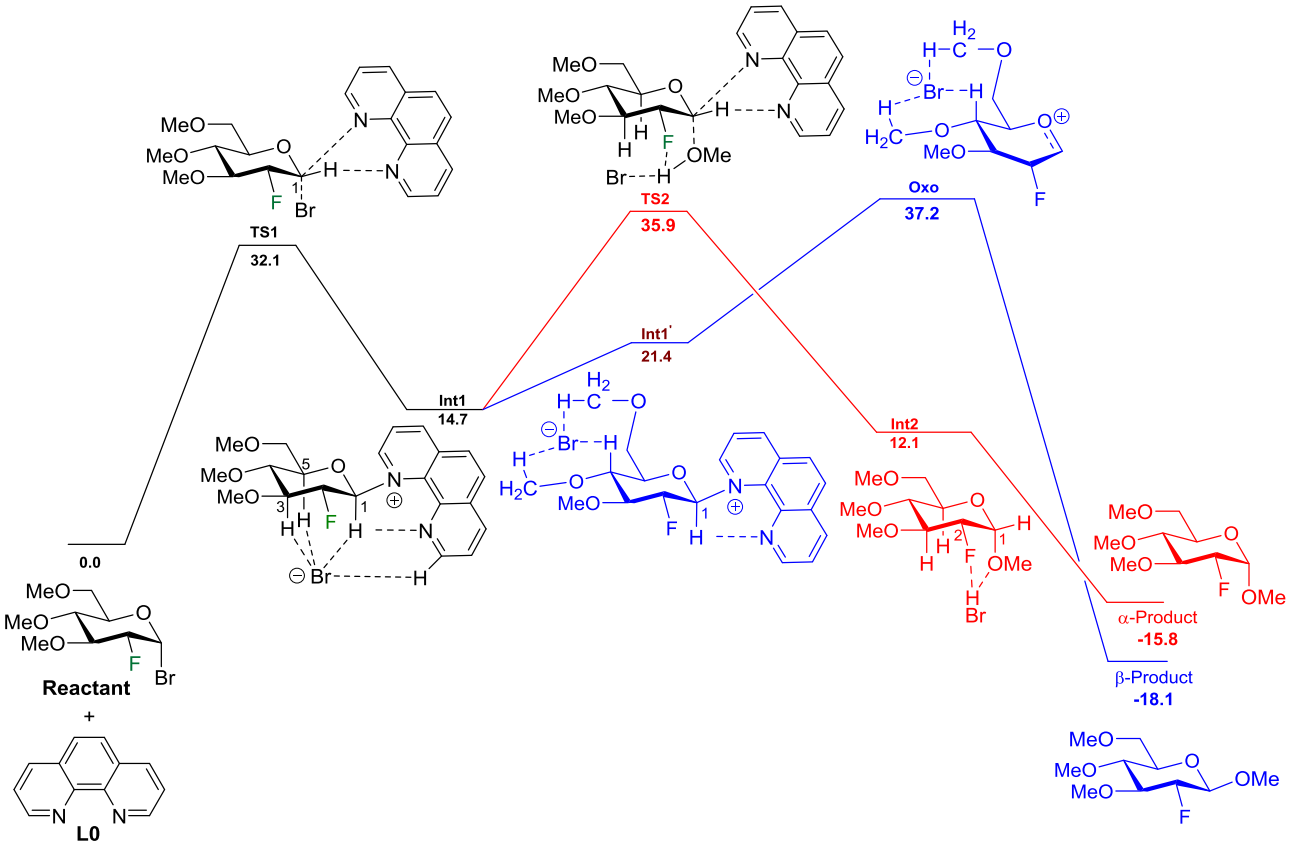


**Figure 4.** Reaction coordinate diagrams showing the diverging pathways for the formation of $\alpha$- (red) and $\beta$- (blue) glycosylation product using phenathroline **L0** as a catalyst as it results in lower glycosylation selectivity than **L1** and **L3**. Also see Figure S1 for calculations of pyridine **L10** as a catalyst.

than the corresponding ones for phenanthroline catalysts (see **L6** in Figure 3). We hypothesized that the differences in the energies of **Int1** between the phenanthroline catalysts and the pyridine catalysts are likely due to steric interactions. The bulky phenanthrolines are higher in energy and have longer C−N bonds (see the Supporting Information) than the pyridine catalysts. The increased steric bulk of the phenanthroline catalysts seems to outweigh any C−H···N hydrogen bonding, which is enough to explain the phenanthroline/pyridine bind energy differences. We hypothesized that this also makes the reverse barriers for **TS1** lower and may result in more of **Int1** returning to reactants and more of the reactants recovered for the phenanthroline catalysts (Table 1, entries 1−9). In contrast, **Int1** of pyridine-based catalysts (**L6**−**L10**) is less likely to reverse to reactants because the reverse barriers for **TS1** are significantly larger than those of phenanthroline catalysts (**L1**−**L5**). This is consistent with our observed experimental data (Table 1, entries 10−13) that a low amount of glucosyl bromide starting material **1** recovered at the end of the reaction for pyridine-based catalysts. It is observed in **TS2** that the C2-fluoride of the sugar and the bromide interact with the hydrogen of methanol. Furthermore, substituents on the phenanthrolines and the pyridines lower both **TS1** and **TS2** (see the Supporting Information), suggesting that the substituted catalysts should be better than the unsubstituted catalysts. For the formation of the $\alpha$-glycoside linkage in the second step, the alcohol group (in this case modeled by methanol) displaces the catalyst in an $S_N2$ manner, with the bromide accepting the proton from the alcohol (Figure 3). In the second intermediate, **Int2**, hydrogen bromide (HBr) is hydrogen-bonded to the C1-oxygen and the C2-fluorine. In the final step, IBO reacts with HBr. The overall reaction is exergonic by 16.4 kcal/mol. For all of the catalysts considered, the barriers relative to separated reactants are 25−35 kcal/mol, in accord with the thermal conditions needed for the reaction.

Although phenanthroline catalysts selectively favor the $\alpha$-1,2-cis glycosylation products, some coupling partners result in low to moderate $\alpha$-selectivities. As a result, computational studies into a mechanism for the $\beta$-selective glycosylation determined a likely divergence point of the $\alpha$- and $\beta$-pathways at the first intermediate, **Int1**, after $S_N2$ attack by the catalyst (Figure 4). Complete dissociation of $Br^-$ ion from the intermediate is not energetically feasible due to the use of the nonpolar solvent MTBE (75.1 kcal/mol), and dissociation of catalyst from **Int1** will lead to the rapid collapse back to reactants due to the proximity of $Br^-$ ion to the generated phenanthrolinium cation. However, migration of $Br^-$ ion away from the anomeric carbon of **Int1** is quite feasible, ultimately forming the species designated **Int1′** (Figure 4). Subsequent dissociation of catalyst from **Int1′** yields a metastable oxocarbenium species (**Oxo**) with a free energy greater than but comparable to that of the second $S_N2$ reaction of the main pathway. Nucleophilic attack on the C1-anomeric carbon of the oxocarbenium can then lead to the formation of either the $\alpha$- or $\beta$-product. Thus, we can expect that the formation of the $\beta$-product to be possible under phenanthroline-catalyzed conditions, but the production of the $\alpha$-anomer should dominate. The calculated difference in free energy for the rate-limiting species is 1.3 kcal/mol. Assuming the **Oxo** intermediate produces an equal amount of each anomer, this


https://dx.doi.org/10.1021/acscatal.0c04381
ACS Catal. 2021, 11, 2108−2120

would lead to a 19:1 $\alpha/\beta$ product ratio. This result indicates that low to moderate selectivities in some coupling products are likely due to the nature of the coupling partners.

## CONCLUSIONS

An efficient method for the stereoselective formation of $\alpha$-1,2-*cis*-2-fluoro glycosides utilizing phenanthroline-based catalysts **L1** and **L3** has been established. **L3** is more effective than **L1** at promoting the coupling to provide the desired $\alpha$-1,2-*cis*-fluorinated glycoside products in higher yield and selectivity. The Gilmour group demonstrated a preference for the formation of $\beta$-1,2-*trans*-2-fluoro glycosides using trihaloacetimidate donors.[15−18] By the use of glycosyl halides and phenanthroline as a catalyst, we have been able to invert the selectivity of the glycosidic bond formation. We hypothesize that the $\alpha$-selectivity is partly due to a double $S_N2$ inversion mechanism promoted by phenanthroline catalyst. With the intention to better understand the mechanism of this catalytic glycosylation system, dinitrogen (phenanthroline type) and mononitrogen (pyridine type) catalysts were evaluated. The reaction yields and the stereoselectivity of the pyridine vs phenanthroline catalysts were rather consistent. The major difference found in the catalytic system was the amount of starting glycosyl halides recovered. In the case of the pyridine catalysts, the amount of recovered donor was significantly less in comparison to that of the phenanthroline catalysts. The substantial amount of starting glycosyl bromide recovered, in combination with less formation of byproducts, suggests that the phenanthroline catalysts allow a more mild form of activation, resulting in a more efficient glycosylation.

## ASSOCIATED CONTENT

### Supporting Information

The Supporting Information is available free of charge at https://pubs.acs.org/doi/10.1021/acscatal.0c04381.

Full experimental procedures and characterization data for all new compounds (PDF)

DFT calculation energies for **L0**−**L10** catalysts (PDF)

## AUTHOR INFORMATION


### Corresponding Authors

**H. Bernhard Schlegel** − *Department of Chemistry, Wayne State University, Detroit, Michigan 48202, United States;* orcid.org/0000-0001-7114-2821; Email: hbs@chem.wayne.edu

**Hien M. Nguyen** − *Department of Chemistry, Wayne State University, Detroit, Michigan 48202, United States;* orcid.org/0000-0002-7626-8439; Email: hmnguyen@wayne.edu

### Authors

**Paul M. DeMent** − *Department of Chemistry, Wayne State University, Detroit, Michigan 48202, United States;* orcid.org/0000-0002-6487-727X

**Chenlu Liu** − *Department of Chemistry, Wayne State University, Detroit, Michigan 48202, United States*

**Joseph Wakpal** − *Department of Chemistry, Wayne State University, Detroit, Michigan 48202, United States*

**Richard N. Schaugaard** − *Department of Chemistry, Wayne State University, Detroit, Michigan 48202, United States*

Complete contact information is available at: https://pubs.acs.org/10.1021/acscatal.0c04381

### Author Contributions

[†]C.L., J.W., and R.N.S. contributed equally.


### Notes

The authors declare no competing financial interest.

## ACKNOWLEDGMENTS

This research is supported by NIH (U01GM120293, R01GM098285, and R01GM136968 for H.M.N.) and NSF (CHE1856437 for H.B.S.). The authors thank the Wayne State University Lumigen Center for instrumental assistance and the Wayne State University Grid for computing resources.

## REFERENCES


(1) Stallforth, P.; Lepenies, B.; Adibekian, A.; Seeberger, P. H. Carbohydrates: a Frontier in Medicinal Chemistry. *J. Med. Chem.* **2009**, *52*, 5561−5577.

(2) Bertozzi, C. R.; Kiessling, L. L. Chemical Glycobiology. *Science* **2001**, *291*, 2357−2364.

(3) Isbell, H. S. Nomenclature of the Alpha and Beta Sugars. *J. Chem. Educ.* **1935**, *12*, No. 96.

(4) Boons, G.-J. Recent Developments in Chemical Oligosaccharide Synthesis. *Contemp. Org. Synth.* **1996**, *3*, 173−200.

(5) Nigudkar, S. S.; Demchenko, A. V. Stereocontrolled 1,2-cis Glycosylation as the Driving Force of Progress in Synthetic Carbohydrate Chemistry. *Chem. Sci.* **2015**, *6*, 2687−2704.

(6) Barnes-Seeman, D.; Beck, J.; Springer, C. Fluorinated Compounds in Medicinal Chemistry: Recent Applications, Synthetic Advances and Matched-Pair Analyses. *Curr. Top. Med. Chem.* **2014**, *14*, 855−864.

(7) Filler, R.; Saha, R. Fluorine in Medicinal Chemistry: a Century of Progress and a 60-Year Retrospective of Selected Highlights. *Future Med. Chem.* **2009**, *1*, 777−791.

(8) Kirk, K. L. Fluorine in Medicinal Chemistry: Recent Therapeutic Applications of Fluorinated Small Molecules. *J. Fluorine Chem.* **2006**, *127*, 1013−1029.

(9) Kirk, K. L. Fluorination in Medicinal Chemistry: Methods, Strategies, and Recent Developments. *Org. Process Res. Dev.* **2008**, *12*, 305−321.

(10) Ojima, I. Use of Fuorine in the Medicinal Chemistry and Chemical Biology of Bioactive Compounds - a Case Study on Fluorinated Taxane Anticancer Agents. *ChemBioChem* **2004**, *5*, 628−635.

(11) Böhm, H.-J.; Banner, D.; Bendels, S.; Kansy, M.; Kuhn, B.; Müller, K.; Obst-Sander, U.; Stahl, M. Fluorine in Medicinal Chemistry. *ChemBioChem* **2004**, *5*, 637−643.

(12) Purser, S.; Moore, P. R.; Swallow, S.; Gouverneur, V. Fluorine in Medicinal Chemistry. *Chem. Soc. Rev.* **2008**, *37*, 320−330.

(13) Vincent, S. P.; Burkart, M. D.; Tsai, C.-Y.; Zhang, Z.; Wong, C.-H. Electrophilic Fluorination−Nucleophilic Addition Reaction Mediated by Selectfluor: Mechanistic Studies and New applications. *J. Org. Chem.* **1999**, *64*, 5264−5279.

(14) Burkart, M. D.; Vincent, S. P.; Wong, C.-H. An Efficient Synthesis of CMP-3-Fluoroneuraminic Acid. *Chem. Commun.* **1999**, 1525−1526.

(15) Bucher, C.; Gilmour, R. Fluorine-Directed Glycosylation. *Angew. Chem., Int. Ed.* **2010**, *49*, 8724−8728.

(16) Durantie, E.; Bucher, C.; Gilmour, R. Fluorine-Directed Beta-Galactosylation: Chemical Glycosylation Development by Molecular Editing. *Chem. − Eur. J.* **2012**, *18*, 8208−8215.

(17) Santschi, N.; Gilmour, R. Comparative Analysis of Fluorine-Directed Glycosylation Selectivity: Interrogating C2 [OH -> F] Substitution in D-Glucose and D-Galactose. *Eur. J. Org. Chem.* **2015**, *2015*, 6983−6987.

(18) Aiguabella, N.; Holland, M. C.; Gilmour, R. Fluorine-Directed 1,2-*trans* Glycosylation of Rare Sugars. *Org. Biomol. Chem.* **2016**, *14*, 5534−5538.

(19) Yu, F.; Li, J. Y.; DeMent, P. M.; Tu, Y. J.; Schlegel, H. B.; Nguyen, H. M. Phenanthroline-Catalyzed Stereoretentive Glycosylations. *Angew. Chem., Int. Ed.* **2019**, *58*, 6957−6961.
(20) Meloncelli, P. J.; Martin, A. D.; Lowary, T. L. Glycosyl Iodides. History and Recent Advances. *Carbohydr. Res.* **2009**, *344*, 1110−1122.
(21) Gervay-Hague, J. Taming the Reactivity of Glycosyl Iodides to Achieve Stereoselective Glycosidation. *Acc. Chem. Res.* **2016**, *49*, 35−47.
(22) Gervay, J.; Hadd, M. J. Anionic Additions to Glycosyl Iodides: Highly Stereoselective Syntheses of Beta-*C*-, *N*-, and *O*-Glycosides. *J. Org. Chem.* **1997**, *62*, 6961−6967.
(23) Gervay, J.; Nguyen, T. N.; Hadd, M. J. Mechanistic Studies on the Stereoselective Formation of Glycosyl Iodides: First Characterization of Beta-D-Glycosyl Iodides. *Carbohydr. Res.* **1997**, *300*, 119−125.
(24) Bhat, A. S.; Gervay-Hague, J. Efficient Syntheses of Betacyanosugars Using Glycosyl Iodides Derived from Per-*O*-Silylated Mono- and Disaccharides. *Org. Lett.* **2001**, *3*, 2081−2084.
(25) Lam, S. N.; Gervay-Hague, J. Efficient Route to 2-Deoxy Beta *O*-Aryl-D-Glycosides via Direct Displacement of Glycosyl Iodides. *Org. Lett.* **2003**, *5*, 4219−4222.
(26) Klyosov, A. A. Carbohydrates and Drug Design: What Is New in This Book. In *ACS Symposium Series*; American Chemical Society, 2006; Vol. *932*, pp 2−24.
(27) Lemieux, R. U.; Morgan, A. R. The Mechanism for the Formation of 1,2-*cis*-Pyridine Nucleosides from 1,2-*cis*-Acetohalogenosugars. A Novel Rearrangement. *J. Am. Chem. Soc.* **1963**, *85*, 1889−1890.
(28) Lemieux, R. U.; Morgan, A. R. The Abnormal Conformations of Pyridinium α-Glycopyranosides. *Can. J. Chem.* **1965**, *43*, 2205−2213.
(29) Becke, A. D. Density-Functional Exchange-Energy Approximation with Correct Asymptotic Behavior. *Phys. Rev. A* **1988**, *38*, No. 3098.
(30) Becke, A. D. Density-Functional Thermochemistry. III. The Role of Exact Exchange. *J. Chem. Phys.* **1993**, *98*, 5648−5652.
(31) Becke, A. D. A New Mixing of Hartree−Fock and Local Density Functional Theories. *J. Chem. Phys.* **1993**, *98*, 1372−1377.
(32) Lee, C.; Yang, W.; Parr, R. G. Development of the ColleSalvetti Correlation-Energy Formula into a Functional of the Electron Density. *Phys. Rev. B* **1988**, *37*, No. 785.
(33) Vosko, S. H.; Wilk, L.; Nusair, M. Accurate Spin-Dependent Electron Liquid Correlation Energies for Local Spin Density Calculations: a Critical Analysis. *Can. J. Phys.* **1980**, *58*, 1200−1211.
(34) Schäfer, A.; Horn, H.; Ahlrichs, R. Fully Optimized Contracted Gaussian Basis Sets for Atoms Li to Kr. *J. Chem. Phys.* **1992**, *97*, 2571−2577.
(35) Grimme, S.; Antony, J.; Ehrlich, S.; Krieg, H. A Consistent and Accurate ab Initio Parametrization of Density Functional Dispersion Correction (DFT-D) for the 94 Elements H-Pu. *J. Chem. Phys.* **2010**, *132*, No. 154104.
(36) Johnson, E. R.; Becke, A. D. A Post-Hartree-Fock Model of Intermolecular Interactions: Inclusion of Higher-Order Corrections. *J. Chem. Phys.* **2006**, *124*, No. 174104.
(37) Marenich, A. V.; Cramer, C. J.; Truhlar, D. G. Universal Solvation Model Based on Solute Electron Density and on a Continuum Model of the Solvent Defined by the Bulk Dielectric Constant and Atomic Surface Tensions. *J. Phys. Chem. B* **2009**, *113*, 6378−6396.
(38) Weigend, F.; Ahlrichs, R. Balanced Basis Sets of Split Valence, Triple Zeta Valence and Quadruple Zeta Valence Quality for H to Rn: Design and Assessment of Accuracy. *Phys. Chem. Chem. Phys.* **2005**, *7*, 3297−3305.
(39) Frisch, M. J.; Trucks, G. W.; Schlegel, H. B.; Scuseria, G. E.; Robb, M. A.; Cheeseman, J. R.; Scalmani, G.; Barone, V.; Petersson, G. A.; Nakatsuji, H.; Li, X.; Caricato, M.; Marenich, A. V.; Bloino, J.; Janesko, B. G.; Gomperts, R.; Mennucci, B.; Hratchian, H. P.; Ortiz, J. V.; Izmaylov, A. F.; Sonnenberg, J. L.; Williams-Young, D.; Ding, F.; Lipparini, F.; Egidi, F.; Goings, J.; Peng, B.; Petrone, A.; Henderson, T.; Ranasinghe, D.; Zakrzewski, V. G.; Gao, J.; Rega, N.; Zheng, G.; Liang, W.; Hada, M.; Ehara, M.; Toyota, K.; Fukuda, R.; Hasegawa, J.; Ishida, M.; Nakajima, T.; Honda, Y.; Kitao, O.; Nakai, H.; Vreven, T.; Throssell, K.; Montgomery, J. A., Jr.; Peralta, J. E.; Ogliaro, F.; Bearpark, M. J.; Heyd, J. J.; Brothers, E. N.; Kudin, K. N.; Staroverov, V. N.; Keith, T. A.; Kobayashi, R.; Normand, J.; Raghavachari, K.; Rendell, A. P.; Burant, J. C.; Iyengar, S. S.; Tomasi, J.; Cossi, M.; Millam, J. M.; Klene, M.; Adamo, C.; Cammi, R.; Ochterski, J. W.; Martin, R. L.; Morokuma, K.; Farkas, O.; Foresman, J. B.; Fox, D. J. *Gaussian 16*, revision B.01; Gaussian, Inc.: Wallingford, CT, 2016.


https://dx.doi.org/10.1021/acscatal.0c04381
*ACS Catal.* 2021, 11, 2108−2120